



Cite this: *Phys. Chem. Chem. Phys.*, 2022, 24, 16852

Three-photon-induced singlet excited-state absorption for tunable ultrafast optical-limiting in distyrylbenzene: a first-principles study†

Danyang Zhang,^a Hongjuan Zhu,^a Chunrui Wang,^b Shuying Kang,^c Yong Zhou ^a and Xiaowei Sheng *^a

The ground and first singlet excited state absorption in distyrylbenzene (DSB) is simulated based on linear-response time dependent density functional theory (LR-TDDFT). It is found that distyrylbenzene shows a strong reverse saturable absorption effect around the near-infrared range. Combining the calculations of cubic response functions to simulate the three-photon absorption in distyrylbenzene, we are able to show that distyrylbenzene is a promising ultrafast optical limiter for the light with wavelengths around 775 nm. The primary mechanism for the optical limiting behavior can be well understood by the three-photon induced excited state absorption (3PA-ESA). This result in that DSB has high transmittance for low-intensity ambient light levels and the ultrafast response of optical-limiting. In addition, the limited optical window can be tuned by changing the length of the π -electron conjugated structure. It was also discovered that the molecular aggregation has an inhibitory effect on the optical limiting efficiency of distyrylbenzene. The present results may serve as a theoretical guideline for the design of distyrylbenzene-based optical limiting materials.

Received 15th April 2022,
Accepted 16th June 2022

DOI: 10.1039/d2cp01753a

rsc.li/pccp

I Introduction

With the rapid development of pulsed intense laser sources, products capable of protecting light-sensitive objects (such as eyes and skin) are increasingly in demand.^{1–3} The materials possessing optical-limiting (OL) properties are useful for laser protection, which show a strong attenuation of light transmission at high input intensities but have a very high transmittance for the light at low input intensities. Accordingly, these materials can be used to protect light-sensitive objects from the damage of intense light radiation without a compromise of linear transmittance. The investigations of optical-limiting materials have thus attracted great attention from researchers in recent decades.^{4–11}

It has been well known that reversed saturable absorption (RSA) is one of the most important mechanisms for the optical-limiting effect. Contrary to the saturable absorption (SA), the absorption coefficient increases with increasing light intensity in the RSA. RSA is a typical nonlinear absorption, which is due to the absorption cross sections of the excited-state that are larger than that of the ground state for the input light.^{12–16} Consequently, both ground and excited state absorption are important for understanding optical-limiting effects.^{17–21}

To date, most studies on optical-limiting properties were based on the ultrafast transient absorption and Z-scan experiment.^{22,23} Within these experiments, the ground and the excited-state absorption (ESA) can both be obtained by decomposing the transient spectrum.^{24–27} However, the interpretation of such spectra can be difficult if these contributions occur in the same energy window.^{28,29} In this context, the theoretical investigations should play an important role to model the ground and excited state absorption spectra.

In the first-principles calculations, the ground state absorption (GSA) spectra are normally simulated by the linear-response time-dependent density functional theory (LR-TDDFT). This method has been widely used to investigate the GSA.^{30–33} However, the ESA is much less explored. This is partly due to the fact that there is no well developed theoretical method to calculate the ESA. One usually relies on quadratic-response time-dependent density functional theory (QR-TDDFT), in which the oscillator strength

^a Anhui Province Key Laboratory of Optoelectric Materials Science and Technology, Department of Physics, Anhui Normal University, Anhui, Wuhu 241000, China. E-mail: xwsheng@mail.ahnu.edu.cn

^b State Key Laboratory of Laser Interaction with Matter, Changchun Institute of Optics, Fine Mechanics and Physics, Chinese Academy of Science, Changchun 130033, China

^c School of Physics and Electronic Information, Gannan Normal University, Ganzhou 341000, China

† Electronic supplementary information (ESI) available: 1. Multi-photon absorption of DSB simulated by different functionals (Table S1); 2. multi-photon absorption of DSB derivatives simulated by BHandHLYP functional (Table S2); 3. Cartesian coordinates for the lowest energy configuration of DSB, DSB dimer and DSB trimer in S_0 state (Table S3). See DOI: <https://doi.org/10.1039/d2cp01753a>

between two excited states is calculated from the double residues of the quadratic-response function at its poles.^{34,35} However, the computational cost is very expensive, scaling as N^6 , for large molecules.

To avoid the computational difficulty of the ESA based on QR-TDDFT theory, several alternative methods for the ESA have been proposed.^{28,36–41} One of these methods is really appealing, in which the auxiliary wave functions based on Casida's ansatz for the excited states were constructed from LR-TDDFT to calculate the absorption spectra.^{40,42} This method has a similar basic theoretical foundation with the SLR-TDDFT (second linear-response time dependent functional theory) and the sTD-DFT (simplified time-dependent density functional theory) methods which were proposed by Mosquera *et al.*^{37,38} and Wergifosse *et al.*,³⁹ respectively. The validation of this method has been well tested on the systems such as phthalocyanine, distyrylbenzene and 3-methylthiophenes.^{40,44,45} One of the most important advantages of this method over QR-TDDFT is that the computational cost is scaling as only N^4 , which is much cheaper compared with QR-TDDFT. It should also be mentioned that the RT-TDDFT (real-time time-dependent density functional theory) method for the ESA proposed by Fischer *et al.* allows N^3 scaling when local functionals are used.^{28,36} These new methods make theoretical investigations on the optical-limiting effects possible.

Optical-limiting effects have been observed in many organic materials, in particular in molecules with the π -electron conjugated system, such as phthalocyanine and its derivatives.^{15,17,23,46–48} Distyrylbenzene (DSB) also has the π -electron conjugated structure, and the ground and excited-state absorption spectra were well investigated by Oliveira *et al.* in theory and experiment.²⁹ The excited-state absorption of DSB was also investigated by the present group.⁴⁰ The previous experimental spectra reveal that the GSA and the ESA of DSB occur at the wavelengths around the center 3.52 eV (352.3 nm) and 1.67 eV (742.5 nm), respectively. This observation indicates that there is a considerable gap between the main band of the GSA and the ESA. Therefore, the RSA may happen in DSB for the light with wavelengths around 1.67 eV, where the ESA is much larger than the GSA. Then, it could be expected that DSB can be used as the optical-limiting material. However, there are no reported investigations on the optical-limiting properties of DSB both in theory and experiment.

In the present paper, the ground and first singlet excited state absorption in the distyrylbenzene (DSB) spectra are combined to investigate its optical-limiting properties based on purely theoretical calculations. The computation results indicate that distyrylbenzene will show strong reverse saturable absorption for the light with wavelengths around the near-infrared range. Combining the multi-photon absorption simulations, it can be well illustrated that distyrylbenzene is a promising ultrafast optical limiter for the light with a wavelength of around 775 nm.

II Methods and computational details

In the present paper, the simulations of the GSA are based on the linear response time-dependent density functional theory (LR-TDDFT). Then, a method derived from the LR-TDDFT is

applied to calculate the ESA. The most important point in this method is that the excited state wavefunction Ψ_I is constructed as a linear combination of singly excited configurations with the Kohn–Sham orbitals applied,

$$\Psi_I = \sum_{i,a} C_I^{i,a} \Phi_i^a. \quad (1)$$

Based on the Casida's ansatz,⁴² the configuration interaction coefficients $C_I^{i,a}$ can be extracted from the solution of the Casida equation:

$$\begin{pmatrix} \mathbf{A} & \mathbf{B} \\ \mathbf{B} & \mathbf{A} \end{pmatrix} \begin{pmatrix} \mathbf{X} \\ \mathbf{Y} \end{pmatrix} = \Omega \begin{pmatrix} -1 & 0 \\ 0 & 1 \end{pmatrix} \begin{pmatrix} \mathbf{X} \\ \mathbf{Y} \end{pmatrix} \quad (2)$$

where the matrix elements of \mathbf{A} and \mathbf{B} are called the orbital rotation Hessians, which are given by

$$A_{i\alpha\sigma, i' \alpha' \sigma'}(\Omega) = \delta_{ii'} \delta_{\alpha\alpha'} \delta_{\sigma\sigma'} \Omega_{\alpha' i' \sigma'} + K_{i\alpha\sigma, i' \alpha' \sigma'}(\Omega) \quad (3)$$

$$B_{i\alpha\sigma, i' \alpha' \sigma'}(\Omega) = K_{i\alpha\sigma, i' \alpha' \sigma'}(\Omega). \quad (4)$$

$K_{i\alpha\sigma, i' \alpha' \sigma'}(\Omega)$ is the defined coupling-matrix elements. For details of these equations, refer to ref. 42 and 43. It should be emphasized that the configuration interaction coefficients determined in this way make eqn (1) totally different from the normal configuration interaction wavefunction with a single excitation (CIS).⁴⁰ It has been shown by us that the wavefunction constructed in the form of eqn (1) is very good for predicting the ESA, which is much better than the traditional CIS wavefunction.⁴⁰ For details of this method refer to ref. 40 and 45. The TDDFT based quadratic and cubic response theories were used to simulate the multi-photon absorption. The exchange correlation functional named BHandHLYP and the basis set 6-311G(d,p) were used in the computations. The validation of the used functional and basis set has been well illustrated in our previous work,^{40,44} where five different exchange–correlation functionals with different percentages of exact Hartree–Fock components have been checked. It was shown that the functionals with roughly 50% of the HF component are recommended, such as BHandHLYP. On the other hand, the choice of BHandHLYP for the present investigated system was also recommended by Oliveira *et al.*²⁹

In order to compare with the experimental results, the ground and first singlet excited state absorption spectra of DSB are simulated in dioxane solvent with the polarizable continuum model (PCM) applied.²⁹ The absorption spectra were obtained by using the calculated transition oscillator strengths and the excitation energies broadened with the Lorentzian function (FWHM = 0.4 eV). The Gaussian 09 package was used to perform the geometry optimization of DSB.⁴⁹ Based on the geometry of the DSB monomer, 50 conformations to each DSB oligomer generated by the Molclus program were pre-optimized with the dispersion-corrected PM6(PM6-DH+) method using the semi-empirical quantum chemistry MOPAC2016 package.^{50,51} Then, ten conformations with relatively low energies and different geometries were screened out and further optimized at the D3 dispersion corrected B3LYP (B3LYP-D3(BJ)) level with the 6-311G(d,p) basis set through the

Gaussian 09 package to obtain the stable conformations of DSB oligomers. Then the structures for the DSB dimer and trimer with the lowest energy were chosen to investigate the influences of aggregation on the absorption spectra. A modified version of the GAMESS (US) package was used to perform the simulations of the GSA and the ESA in the present system.⁵² The Dalton 2018 program was used to do the quadratic and cubic response calculations.^{53,54} The frontier molecular orbitals analysis, the electron density difference between two singlet excited states, the analysis of transition dipole moment vector contributed by different DSB monomers and the analysis of the interfragment charge transfer (IFCT) were done by the wavefunction analysis program Multiwfn.⁵⁵ The IFCT method estimates the amount of electron transfer between two fragments by calculating the contributions of the two fragments to the hole and electron, respectively. For more discussion of the IFCT method, refer to ref. 56. The electrostatic potential involved in the analyses was evaluated by Multiwfn based on the highly effective algorithm proposed in ref. 57. Finally, these calculations and analysis results were visualized through the VMD package.⁵⁸

III Results and discussion

A. Ground state absorption, the first singlet excited-state absorption and reverse saturable absorption in DSB

The structure optimization reveals that DSB has C_{2h} symmetry, which is consistent with the previous result.²⁹ The calculated absorption spectra of the ground state (black dash-dotted line) and first singlet excited state (blue dashed line) of DSB are shown in Fig. 1. For comparison, the positions with prominent absorption observed in the experiment are also shown in Fig. 1 (green vertical dashed lines).²⁹ The present predicted peak position of the GSA spectrum is 3.51 eV, which is in excellent agreement with the experimental observation (3.52 eV). For the

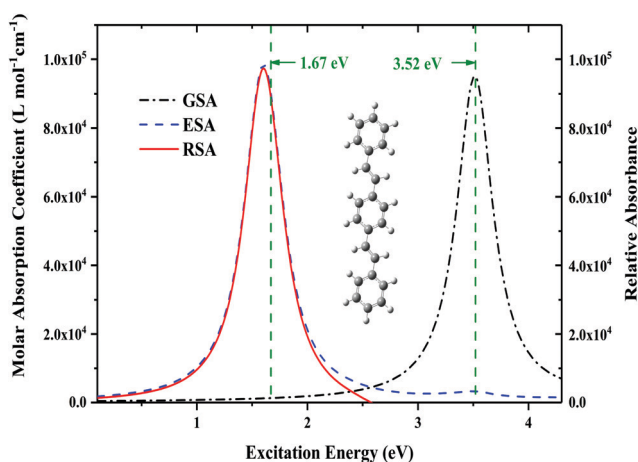


Fig. 1 Simulated absorption spectra of DSB in the ground state S_0 (black dash-dotted line) and first singlet excited state S_1 (blue dashed line). The vertical dashed lines are the experimental results which are taken from ref. 29. The red line is the relative absorbance which is defined as the difference between the ESA and the GSA. A red curve with a value above zero means that the ESA is greater than the GSA.

peak position of the ESA spectrum, the present result is 1.60 eV, which is only underestimated by 0.07 eV compared to the experimental measurement at 1.67 eV.²⁹ These observations illustrate that the present theoretical method is very good for the simulations of the GSA and the ESA in DSB.

Now let's focus on the characteristics of electron excitations in the GSA and the ESA. Most of the details are shown in Fig. 2. For the GSA, it can be found from Fig. 2 that the main transition is $S_0 (1^1A_g) \rightarrow S_1 (1^1B_u)$, which can be well characterized by a single transition from the highest occupied to the lowest unoccupied molecular orbital (HOMO \rightarrow LUMO). The electron density difference calculations as shown in Fig. 2 reveal that this is a local excitation. The electron excitations occur mainly inside the three rings of benzene. These observations are perfectly in agreement with the previous results.^{29,59} Both $S_1 (1^1B_u) \rightarrow S_4 (3^1A_g)$ and $S_1 (1^1B_u) \rightarrow S_6 (4^1A_g)$ transitions are important for the ESA as shown in Fig. 2. These two excited states (S_4 and S_6) cannot be characterized by a single configuration. At least six configurations have to be included to describe these excited-states. For the transition $S_1 \rightarrow S_4$, the charge transfer characters can be observed as shown in Fig. 2. Noticeable electron densities transfer to the green regions on the central benzene ring and two double bonds from the blue regions on the two edge benzene rings. However, this is not the case for the transition $S_1 \rightarrow S_6$, which is a local excitation just as the transition $S_0 \rightarrow S_1$ in the GSA. For a more elaborate discussion about the electronic structures of the excited-states involved in the GSA and ESA spectra we refer to ref. 29, where the vibronic analysis was also performed to reveal the ESA features.

The above determined GSA and ESA enable us to discuss the RSA properties in DSB. As we have shown in the above paragraph, the prominent absorption of the GSA and the ESA in DSB is around 3.51 eV and 1.60 eV, respectively. This reveals that there is a considerable gap (1.91 eV) between the main bands of the GSA and the ESA in DSB. Fig. 1 also displays the curve of relative absorbance (red solid line), which is defined as the differences between the ESA and the GSA. It is clearly shown that the ESA is greater than the GSA for the light with a wavelength of around 775 nm (1.60 eV). Therefore, the present theoretical calculations indicate that the reverse saturable absorption (RSA) occurs for the light with wavelengths around 775 nm (1.60 eV).

B. Ultrafast optical-limiting effect in DSB

As we have shown in the above section, DSB shows reverse saturable absorption for the light with a wavelength of around 775 nm. It should be mentioned that this effect can only be activated when the electrons are promoted to the first singlet excited state (S_1) from the ground state (S_0). However, 775 nm is far away from the resonant absorption band 353 nm (3.51 eV) of the GSA. The normal single photon absorption is not possible to fit this requirement.

Fortunately, the previous investigations reveal that the multi-photon absorption is also possible in DSB.^{60–62} Therefore, we also performed the simulations of two-photon and three-

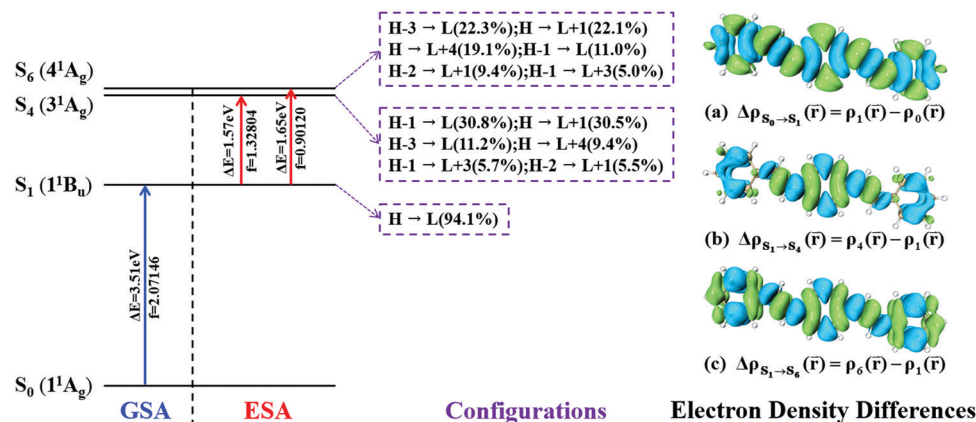


Fig. 2 The left column displays the main transitions involved in the GSA and the ESA. The configurations of the excited-state involved in the GSA and the ESA, which are shown in the middle column. The right column shows the electron density differences between the states involved in the transitions of the GSA and the ESA. Blue and green regions show the decrease and increase of the electron density, respectively. The iso-surface value is fixed to 0.0002 \AA^{-3} .

photon absorption in DSB for the lowest six singlet excited states. The results are shown in Table 1. It is clearly shown that the transitions from S_0 to the singlet excited-state S_1 and S_3 can occur with quite a high transition probability through the three-photon absorption for the wavelength 1025 nm (1.21 eV) and 765 nm (1.62 eV). This indicates that the light with wavelengths around 765 nm and 1025 nm can be absorbed to promote the electrons from the ground state to the excited-state S_1 or S_3 . The excited molecules in the state of S_3 have the tendency to rapidly relax to the lowest vibrational sub-level of the metastable state S_1 through the internal conversion and vibrational relaxation. It has been shown in Fig. 1 that the light with a wavelength of around 775 nm can also be absorbed by DSB in the excited-state S_1 . Accordingly, the electrons excited to the S_1 state through three-photon absorption will absorb one more photon transition to higher levels. Here the molecules decaying to the ground state S_0 from S_1 are neglected as we assume that the pulse width of the laser is much shorter than the relaxation time. As for the calculations of multi-photon absorption, in addition to the presently discussed BHandHLYP, we also checked two different exchange–correlation functionals, B3LYP and CAM-B3LYP. The results are shown in the ESI† (Table S1). It is expected that due to their different percentage of exact Hartree–Fock components, the excitation energies simulated by different functionals are different. However, all of these results enable us to illustrate that the

optical limiting effect in DSB could be achieved through three-photon induced excited state absorption (3PA-ESA).

With the above observations, an optical limiter based on the three-photon induced excited state absorption can be designed for the light with a wavelength of around 775 nm. A schematic diagram for the optical limiter based on DSB is shown in Fig. 3. This optical limiter is attractive because of the following advantages. Firstly, it has a high linear transmittance for the limited wavelength of 775 nm as it is far away from the resonant absorption band of the GSA. For the light with wavelengths around 775 nm, the DSB will strongly attenuate intense optical beams while exhibiting high transmittance for low-intensity ambient light levels. Secondly, the response time toward ultrafast pulses is very short since the intersystem crossing process is not needed (the intersystem crossing time is usually in the nanosecond time scale⁶³). The response time of the present discussed optical limiter is not limited to the intersystem crossing, which only depends on the time of the excited-state S_3 relax to the first singlet excited-state S_1 . This process occurs usually in the picosecond time scale.³ Thirdly, the present theoretically predicted optical-limiting window for DSB is around 775 nm, which is different from phthalocyanine and its derivatives.³⁶ It is noticed that the biological materials and atmosphere have a low absorption coefficient at this wavelength, therefore the light with this wavelength has many potential applications in fields such as military, industry and

Table 1 Excitation energy ΔE , 2PA energy E_{2PA} , 2PA transition probability δ_{2PA} , 3PA energy E_{3PA} and 3PA transition probability δ_{3PA} for linear polarized light of the lowest six singlet excited states of the DSB molecule in vacuum at the BHandHLYP/6-311G(d,p) level

State	ΔE		E_{2PA}		δ_{2PA}	E_{3PA}		δ_{3PA}
	eV	nm	eV	nm	a. u.	eV	nm	a. u.
S_1 (1^1B_u)	3.64	340.66	1.82	681.32	0.00	1.21	1024.79	9.74×10^8
S_2 (2^1A_g)	4.77	259.96	2.39	518.83	1.21×10^3	1.59	779.87	0.00
S_3 (2^1B_u)	4.85	255.67	2.43	510.29	0.00	1.62	765.43	2.46×10^7
S_4 (3^1A_g)	5.09	243.61	2.55	486.27	1.94×10^5	1.70	729.41	0.00
S_5 (3^1B_u)	5.12	242.19	2.56	484.38	0.00	1.71	725.15	6.99×10^6
S_6 (4^1A_g)	5.17	239.85	2.59	478.76	1.22×10^5	1.72	720.93	0.00

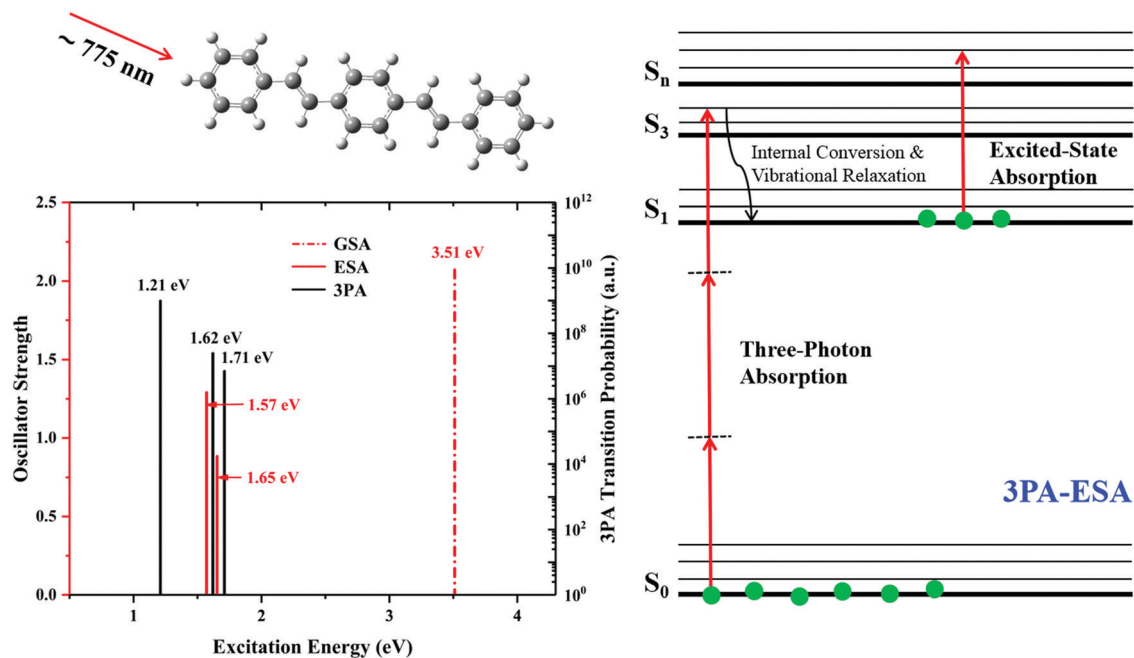


Fig. 3 The optical-limiting effect in DSB. The present theoretical calculations indicate that DSB can be a promising ultrafast optical limiter for the light with a wavelength of around 775 nm. The mechanism can be well understood by three-photon-induced singlet excited-state absorption as shown in the right column.

medical equipment.⁸ It should also be mentioned that Sebastian *et al.*¹⁷ show that the substituted azaphthalocyanines and pyrene-incorporated azaphthalocyanines also show the optical-limiting effects for the femtosecond-scale laser (90 fs) pulses at the near-infrared wavelength of 800 nm due to the two-photon-induced singlet excited-state absorption.

C. Tunable optical-limiting effect in DSB

The optical-limiting window is a critical factor for the application of optical-limiting materials.^{64,65} It is found that the optical-limiting window also can be tuned by changing the length of the π -electron conjugated structure. We designed four derivatives of distyrylbenzene as shown in Fig. 4. These derivatives were designed by reducing or increasing the π -electron conjugated structure in distyrylbenzene named DSB-1, DSB + 1, DSB + 2 and DSB + 3, respectively.

It is clearly shown in Fig. 4 that the GSA and the ESA can be tuned smoothly by changing the length of the π -electron conjugated structure. Increasing the length of the π -electron conjugated structure in distyrylbenzene will result in a red shift for both the GSA and the ESA. This shift becomes smaller and smaller as the length of the π -electron conjugated structure increases. As one can see, the red shift of DSB+3 corresponding to DSB+2 is only 0.09 eV and 0.05 eV for the GSA and the ESA, respectively. With the present investigated four derivatives of DSB, it is found that the position with prominent absorption in DSB can be tuned between 2.97 eV (417.5 nm) and 4.19 eV (295.9 nm) for the GSA, and between 1.26 eV (984.1 nm) and 2.04 eV (607.8 nm) for the ESA. We also performed simulations of 2PA and 3PA for these derivatives, which are listed in the ESI† (Table S2). Both 2PA and 3PA are enhanced with increasing

conjugation length. Combined with the ESA spectra, it can be seen that with the increase of conjugation length, their optical limiting properties have a gradual red-shift. Consequently, the optical-limiting window in DSB can be adjusted as required for actual applications.

D. The influences of aggregation on the GSA and ESA spectra and the optical-limiting Effect in DSB

Due to the planar structure and π -electron conjugated network of DSB, the interaction between DSB monomers is prone to occur, which in turn leads to aggregation.⁶⁶ In particular in organic solvents, the interaction between adjacent DSB monomers is more likely to occur, resulting in coupling between the electronic states of two or more monomers, which changes the photophysical properties of DSB.⁶⁷ In order to determine the influences of aggregation on the photophysical properties of DSB, we constructed the DSB dimer and trimer in dioxane solvent, and compared their GSA and ESA spectra with the results of the DSB monomer. The way to obtain the structures of the DSB dimer and trimer was described in the Methods and Computational section. The structures are shown in Fig. 5(a) and the cartesian coordinates for the structures of these systems in the ground state S_0 are listed in the ESI† (Table S3). The calculated GSA and ESA of DSB and its dimer and trimer are shown in Fig. 5(b). It is clearly shown that the aggregations between DSB monomers result in a blue shift to the excited state absorption, but a red shift to the ground state absorption. Compared with the DSB monomer, the GSA peaks of the dimer and trimer become stronger and wider. However, this is not the case for the ESA. As one can see from Fig. 5, the ESA of the DSB dimer has even been weakened compared with the ESA of the

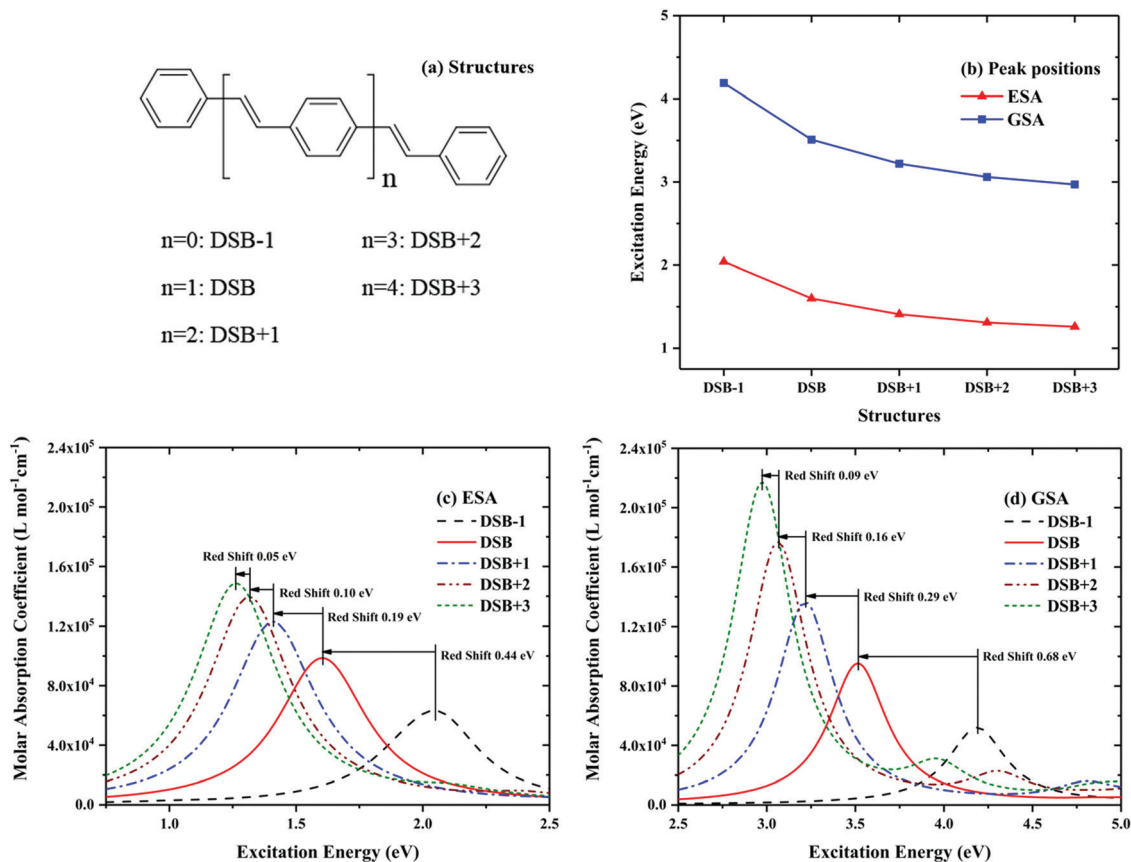


Fig. 4 The ground (S_0) and first singlet excited-state (S_1) absorption in the DSB and its derivatives. (a) The derivatives of DSB are designed by reducing or increasing the length of the π -electron conjugated structure. (b) The positions of the absorption peak for DSB and its derivatives in the ground state (S_0) and the first singlet excited-state (S_1). (c) The absorption spectra for DSB and its derivatives in the first singlet excited-state (S_1). (d) The absorption spectra for DSB and its derivatives in the ground state (S_0).

DSB monomer. This indicates that the molecular aggregation has an inhibitory effect on the optical limiting efficiency of distyrylbenzene.

These changes in the GSA and the ESA can be attributed to the complicated coupling of electronic states between multiple monomers. More details can be found from the analysis of the transition dipole moment, which is one of the critical quantities for the absorption spectra. We analyzed the contribution of each monomer to the transition dipole moment corresponding to the main transitions involved in the GSA and the ESA for the DSB dimer and trimer. Regarding the main transitions in the GSA, the transition dipole moments contributed by each monomer in the DSB dimer or trimer are almost the same, which enhances the absorption of the GSA with the increasing monomer number. For the main transitions involved in the ESA, the contributions of the transition dipole moment from different monomers are different. There is one monomer in the DSB trimer that contributes almost zero to the total transition dipole moment. Accordingly, the strength of the ESA is not enhanced by the monomer aggregation as we have shown in Fig. 6.

The differences in the electron excited characters among the DSB monomer, dimer and trimer may also be expected. It has been shown in Fig. 2 that the main transitions of the GSA for the DSB monomer are local excitations. However, the charge transfer

character was found in the one of the main transitions of the ESA for the DSB monomer. For the DSB dimer and trimer, the electron density differences between the two states involved in the main transitions of the GSA and the ESA are shown in Fig. 7.

As one can see from Fig. 7 (the upper two photos) the charge excited characters of the main transitions in the GSA and the ESA are similar to the DSB monomer for the DSB dimer. The only difference is that the direction of the charge transfer in the main transition of the ESA is from the center to one of the edges in the DSB dimer. In the case of the DSB monomer the charge transfer occurs from the center to the two edges. The bottom two photos of Fig. 7 show the results for the DSB trimer, which reveal that the electron excited characters in the GSA and the ESA are both different from the monomer and dimer. The charge transfer between DSB molecules can be observed for both the GSA and the ESA. This may not be very clear from Fig. 7 for the GSA. The numerical result based on the IFCT analysis of the main transition ($S_0 \rightarrow S_3$) in the GSA reveals that 0.00791 electrons moved from the bottom two DSB molecules to the top DSB. These observations confirm that there is considerable coupling between the electronic states of the two DSB monomers.

It should be mentioned that the aggregations of the DSB monomer may restrain the optical-limiting effect in

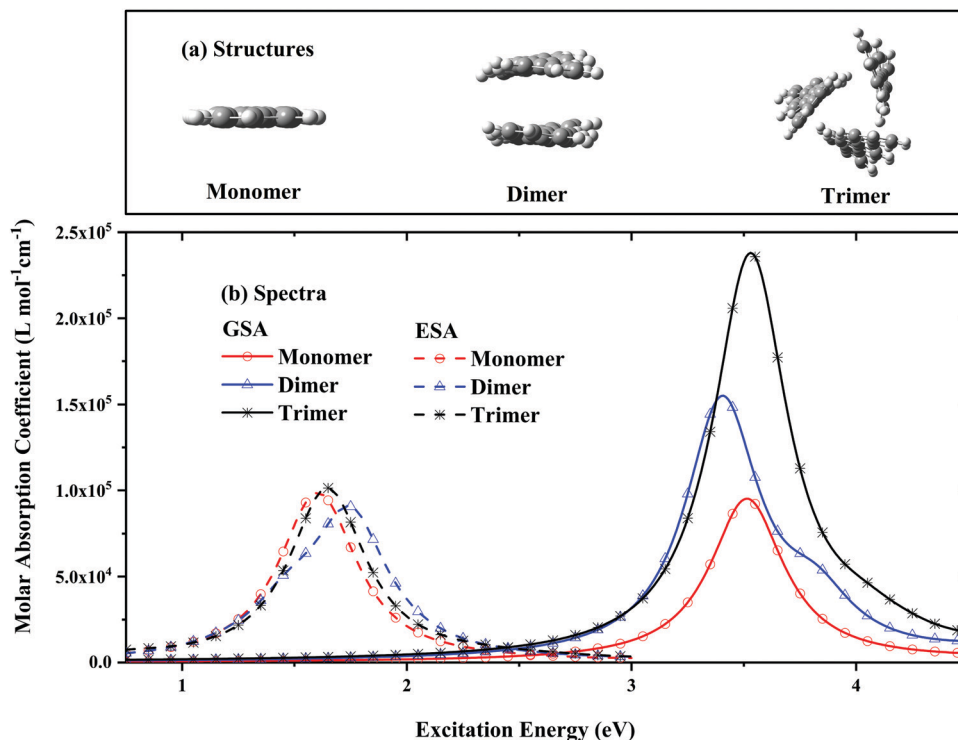


Fig. 5 (a) The structures of the DSB dimer and trimer. These structures are obtained based on the method described in the section named Methods and computational details. (b). The ground (S_0) and first singlet excited-state (S_1) absorption in the DSB and its dimer and trimer.

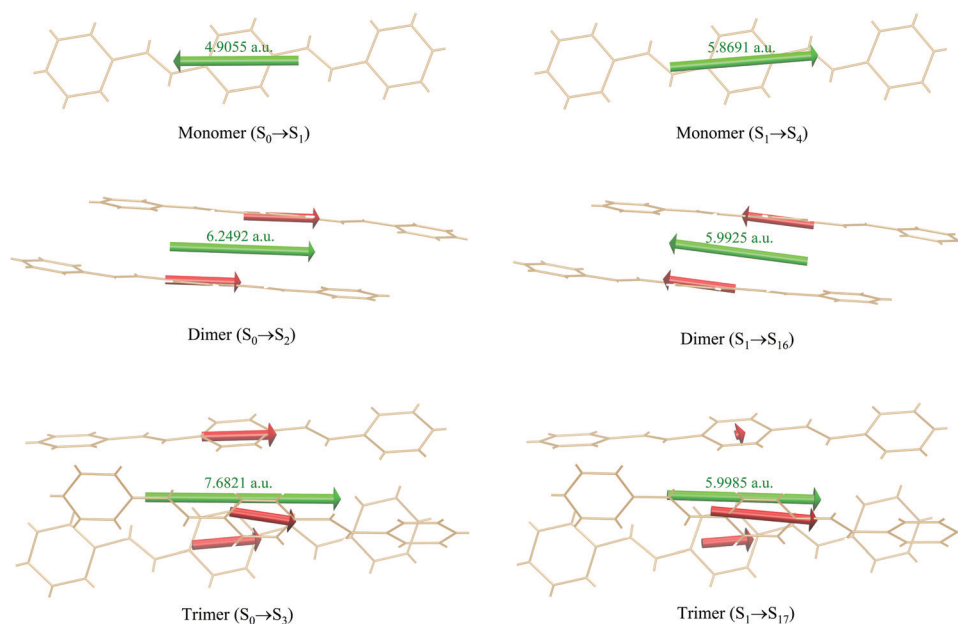


Fig. 6 Transition dipole moment vector contributed by different DSB monomers. The red arrows represent the contribution of each monomer, and the green arrows represent the total transition dipole moment vector of the entire system. The length of the cylindrical part of the arrow corresponds to the size of the transition dipole moment contributed by the fragment, and the direction of the arrow indicates the direction of the transition dipole moment vector.

distyrylbenzene as we have shown in the above sections. A general strategy for this issue is that adding appropriate ligand groups to the molecules may effectively inhibit the molecular aggregation. For the present system DSB, this kind

of molecular decoration can be done easily. Fig. 8 displays the electrostatic potential map (EPM) of DSB. It is clearly shown the possible sites for nucleophilic attack localized over the hydrogen atom.

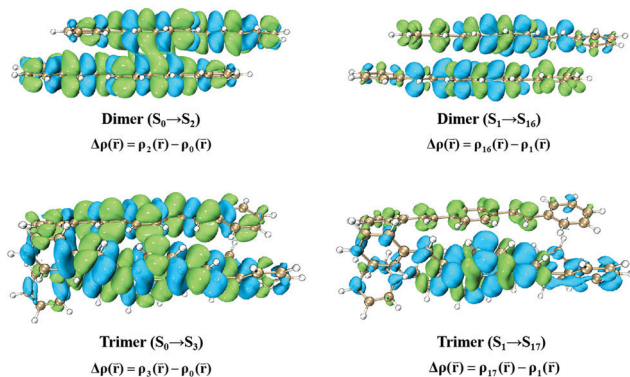


Fig. 7 The electron density differences between the two states involved in the main transitions of the GSA and the ESA, respectively, for the DSB dimer and trimer. Blue and green regions show the decrease and increase of the electron density respectively. The iso-surface value is fixed to 0.0002 \AA^{-3} .

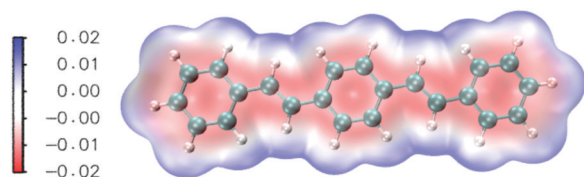


Fig. 8 The electrostatic potential map of DSB calculated with the BHandHLYP/6-311G(d,p) functional. The blue color indicates the maximum positive region making the site favorable for a nucleophilic attack while the red color represents the maximum negative region promoting the site for electrophilic attack.

IV Conclusions

In the present paper, the first-principles calculations based on the linear-response theory were performed to simulate the ground and the first singlet excited-state absorption in distyrylbenzene. The results indicate that the reverse saturable absorption at wavelengths around 775 nm will occur in distyrylbenzene. The calculations of 3PA by cubic response function reveal that distyrylbenzene is a promising optical limiter for wavelengths around 775 nm. It is also found that the optical-limiting window can be tuned by changing the length of the π -electron conjugated structure in distyrylbenzene. The high linear transmittance, ultrafast response time, and the tunable optical windows are among the advantages of the present predicted optical-limiting material. By analyzing the changes between the simulated ground and singlet excited-state absorption spectra of distyrylbenzene and those of distyrylbenzene oligomers, it is found that the aggregation effect, in particular π - π stacking, weakens the optical limiting effect of distyrylbenzene.

Author contributions

Danyang Zhang: data curation, formal analysis. Hongjuan Zhu: software, validation. Chunrui Wang: conceptualization. Shuying Kang: validation. Yong Zhou: conceptualization. Xiaowei Sheng: methodology, writing-original, supervision, funding acquisition.

Data availability

The data that support the findings of this study are available from the corresponding author (Xiaowei Sheng; E-mail: xwsheng@mail.ahnu.edu.cn) upon reasonable request.

Conflicts of interest

The authors declare no conflict of interest.

Acknowledgements

This work is supported by the National Natural Science Foundation of China (No. 12174003, No. 11864003, and No. 62005276), the Anhui Provincial Natural Science Foundation (No. 2008085MA25), the Institute of Energy, Hefei Comprehensive National Science Center (No. GXXT-2020-004), the Fund of the State Key Laboratory of Laser Interaction with Matter, China (SKLLIM1906), and the Youth Innovation Promotion Association, CAS (2019220).

References

- 1 A. Khalatpour, A. K. Paulsen, C. Deimert, Z. R. Wasilewski and Q. Hu, High-power portable terahertz laser systems, *Nat. Photonics*, 2021, **15**, 16.
- 2 M. Malinauskas, A. Žukauskas, S. Hasegawa, Y. Hayasaki, V. Mizeikis, R. Buividas and S. Juodkakis, Ultrafast laser processing of materials: From science to industry, *Light: Sci. Appl.*, 2016, **5**, e16133.
- 3 G. S. He, L.-S. Tan, Q. Zheng and P. N. Prasad, Multiphoton absorbing materials: Molecular designs, characterizations, and applications, *Chem. Rev.*, 2008, **108**, 1245.
- 4 Y. Li, L. H. Yan, J. H. Si, Z. Z. Liang, W. B. Huang, H. P. Ma and X. Hou, Nonlinear optical limiting property and carrier dynamics in tin phthalocyanine porous organic frameworks, *J. Chem. Phys.*, 2022, **156**, 054702.
- 5 D. J. Li, Q. H. Li, Z. R. Wang, Z. Z. Ma, Z. G. Gu and J. Zhang, Interpenetrated metal-porphyrinic framework for enhanced nonlinear optical limiting, *J. Am. Chem. Soc.*, 2021, **143**, 17162.
- 6 T. Kamatsuki, I. Bhattacharjee and S. Hirata, The substituent-induced symmetry-forbidden electronic transition allows significant optical limiting under weak sky-blue irradiance, *J. Phys. Chem. Lett.*, 2020, **11**, 8675.
- 7 I. Papadakis, M. Stavrou, S. Bawari, T. N. Narayanan and S. Couris, Outstanding broadband (532 nm to 2.2 μm) and very efficient optical limiting performance of some defect-engineered graphenes, *J. Phys. Chem. Lett.*, 2020, **11**, 9515.
- 8 G. Liang, L. Tao, Y. H. Tsang, L. Zeng, X. Liu, J. Li, J. Qu and Q. Wen, Optical limiting properties of a few-layer MoS₂/PMMA composite under excitation of ultrafast laser pulses, *J. Mater. Chem. C*, 2019, **7**, 495.
- 9 J. Sun, B. Yuan, X. Hou, C. Yan, X. Sun, Z. Xie, X. Shao and S. Zhou, Broadband optical limiting of a novel twisted tetrathiafulvalene incorporated donor-acceptor material and its ormosil gel glasses, *J. Mater. Chem. C*, 2018, **6**, 8495.

- 10 J. Jia, X. Wu, Y. Fang, J. Yang, X. Guo, Q. Xu, Y. Han and Y. Song, Ultrafast broad-band optical limiting in simple hydrazone derivatives with a Π -conjugated system: Effect of two-photon-induced singlet-state absorption, *J. Phys. Chem. C*, 2018, **122**, 16234.
- 11 C. Cocchi, D. Prezzi, A. Ruini, E. Molinari and C. A. Rozzi, *Ab initio* simulation of optical limiting: The case of metal-free phthalocyanine, *Phys. Rev. Lett.*, 2014, **112**, 198303.
- 12 M. Diao, H. Li, Y. Sun, Y. Liang, Z. Yu, D. W. Boukhvalov, Z. Huang and C. Zhang, Enhancing reverse saturable absorption in SnS₂ nanosheets by plasma treatment, *ACS Appl. Mater. Interfaces*, 2021, **13**, 4211.
- 13 R. Kumar, A. Kumar, N. Verma, R. Philip and B. Sahoo, Mechanistic insights into the optical limiting performance of carbonaceous nanomaterials embedded with core-shell type graphite encapsulated Co nanoparticles, *Phys. Chem. Chem. Phys.*, 2020, **22**, 27224.
- 14 X. Tian, R. Wei, Q. Guo, Y.-J. Zhao and J. Qiu, Reverse saturable absorption induced by phonon-assisted anti-Stokes processes, *Adv. Mater.*, 2018, **30**, 1801638.
- 15 J. Chen, Y. Xu, M. Cao, Y. Wang, T. Liang, H. Li, S. Wang and G. Yang, Strong reverse saturable absorption effect of a nonaggregated phthalocyanine-grafted MA-VA Polymer, *J. Mater. Chem. C*, 2018, **6**, 9767.
- 16 B. I. Cho, M. S. Cho, M. Kim, H.-K. Chung, B. Barbreil, K. Engelhorn, T. Burian, J. Chalupský, O. Ciricosta and G. L. Dakovski, *et al.*, Observation of reverse saturable absorption of an X-ray laser, *Phys. Rev. Lett.*, 2017, **119**, 075002.
- 17 M. Sebastian, A. Ganesan, H. Behbehani, A. Husain and S. Makhseed, Ultrafast nonlinear optical characteristics of pyrene-conjugated azaphthalocyanines with optical limiting behavior, *J. Phys. Chem. C*, 2020, **124**, 21740.
- 18 H. Su, S. Zhu, M. Qu, R. Liu, G. Song and H. Zhu, 1,3,5-Triazine-based Pt(II) metallogel material: Synthesis, photophysical properties, and optical power-limiting performance, *J. Phys. Chem. C*, 2019, **123**, 15685.
- 19 Y. Bai, J.-H. Olivier, H. Yoo, N. F. Polizzi, J. Park, J. Rawson and M. J. Therien, Molecular road map to tuning ground state absorption and excited state dynamics of long-wavelength absorbers, *J. Am. Chem. Soc.*, 2017, **139**, 16946.
- 20 R. B. Roseli, P. C. Tapping and T. W. Kee, Origin of the excited-state absorption spectrum of polythiophene, *J. Phys. Chem. Lett.*, 2017, **8**, 2806.
- 21 D. N. Bowman, J. C. Asher, S. A. Fischer, C. J. Cramer and N. Govind, Excited-state absorption in tetrapyrrolyl porphyrins: Comparing real-time and quadratic-response time-dependent density functional theory, *Phys. Chem. Chem. Phys.*, 2017, **19**, 27452.
- 22 S. Renken, R. Pandya, K. Georgiou, R. Jayaprakash, L. Cai, Z. Shen, D. C. Lidzey, A. Rao and A. J. Musser, Untargeted effects in organic exciton-polariton transient spectroscopy: A cautionary tale, *J. Chem. Phys.*, 2021, **155**, 154701.
- 23 Q. Bellier, N. S. Makarov, P.-A. Bouit, S. Rigaut, K. Kamada, P. Feneyrou, G. Berginc, O. Maury, J. W. Perry and C. Andraud, Excited state absorption: A key phenomenon for the improvement of biphotonic based optical limiting at telecommunication wavelengths, *Phys. Chem. Chem. Phys.*, 2012, **14**, 15299.
- 24 A. Kaur, T. Goswami, K. J. Babu, N. Ghorai, G. Kaur, A. Shukla, S. R. Rondiya and H. N. Ghosh, Probing ultrafast charge separation in CZTS/CdS heterojunctions through femtosecond transient absorption spectroscopy, *J. Phys. Chem. C*, 2020, **124**, 19476.
- 25 A. Bhattacharjee, K. Schnorr, S. Oesterling, Z. Yang, T. Xue, R. de Vivie-Riedle and S. R. Leone, Photoinduced heterocyclic ring opening of furfural: Distinct open-chain product identification by ultrafast x-ray transient absorption spectroscopy, *J. Am. Chem. Soc.*, 2018, **140**, 12538.
- 26 K. E. Knowles, M. D. Koch and J. L. Shelton, Three applications of ultrafast transient absorption spectroscopy of semiconductor thin films: Spectroelectrochemistry, microscopy, and identification of thermal contributions, *J. Mater. Chem. C*, 2018, **6**, 11853.
- 27 B. Debus, M. Orío, J. Rehaut, G. Burdzinski, C. Ruckebusch and M. Sliwa, Fusion of ultraviolet-visible and infrared transient absorption spectroscopy data to model ultrafast photoisomerization, *J. Phys. Chem. Lett.*, 2017, **8**, 3530.
- 28 S. A. Fischer, C. J. Cramer and N. Govind, Excited state absorption from real-time time-dependent density functional theory, *J. Chem. Theory Comput.*, 2015, **11**, 4294.
- 29 E. F. Oliveira, J. Shi, F. C. Lavarda, L. Lüer, B. Milián-Medina and J. Gierschner, Excited state absorption spectra of dissolved and aggregated distyrylbenzene: A TD-DFT state and vibronic analysis, *J. Chem. Phys.*, 2017, **147**, 034903.
- 30 R. F. Theisen, L. Huang, T. Fleetham, J. B. Adams and J. Li, Ground and excited states of zinc phthalocyanine, zinc tetrabenzoporphyrin, and azaporphyrin analogs using DFT and TDDFT with Franck-Condon analysis, *J. Chem. Phys.*, 2015, **142**, 094310.
- 31 C. Adamo and D. Jacquemin, The calculations of excited-state properties with time-dependent density functional theory, *Chem. Soc. Rev.*, 2013, **42**, 845.
- 32 J. Tao and S. Tretiak, Optical absorptions of new blue-light emitting oligoquinolines bearing pyrenyl and triphenyl end-groups investigated with time-dependent density functional theory, *J. Chem. Theory Comput.*, 2009, **5**, 866.
- 33 N. Marom, O. Hod, G. E. Scuseria and L. Kronik, Electronic structure of copper phthalocyanine: A comparative density functional theory study, *J. Chem. Phys.*, 2008, **128**, 164107.
- 34 P. Salek, O. Vahtras, T. Helgaker and H. Ågren, Density-functional theory of linear and nonlinear time-dependent molecular properties, *J. Chem. Phys.*, 2002, **117**, 9630.
- 35 O. Christiansen, P. Jørgensen and C. Hättig, Response functions from Fourier component variational perturbation theory applied to a time-averaged quasienergy, *Int. J. Quantum Chem.*, 1998, **68**, 1.
- 36 S. A. Fischer, C. J. Cramer and N. Govind, Excited-state absorption from real-time time-dependent density functional theory: Optical limiting in zinc phthalocyanine, *J. Phys. Chem. Lett.*, 2016, **7**, 1387.
- 37 M. A. Mosquera, L. X. Chen, M. A. Ratner and G. C. Schatz, Sequential double excitations from linear-response time-

- dependent density functional theory, *J. Chem. Phys.*, 2016, **144**, 204105.
- 38 M. A. Mosquera, N. E. Jackson, T. J. Fauvell, M. S. Kelley, L. X. Chen, G. C. Schatz and M. A. Ratner, Exciton absorption spectra by linear response methods: Application to conjugated polymers, *J. Am. Chem. Soc.*, 2017, **139**, 3728.
- 39 M. de Wergifosse and S. Grimme, Nonlinear-response properties in a simplified time-dependent density functional theory (sTD-DFT) framework: Evaluation of excited-state absorption spectra, *J. Chem. Phys.*, 2019, **150**, 094112.
- 40 X. Sheng, H. Zhu, K. Yin, J. Chen, J. Wang, C. Wang, J. Shao and F. Chen, Excited-state absorption by linear response time-dependent density functional theory, *J. Phys. Chem. C*, 2020, **124**, 4693.
- 41 J. C. Roldao, E. F. Oliveira, B. Milian-Medina, J. Gierschner and D. Roca-Sanjuan, Quantum-chemistry study of the ground and excited state absorption of distyrylbenzene: Multi vs. single reference methods, *J. Chem. Phys.*, 2022, **156**, 044102.
- 42 M. E. Casida, Time-dependent density-functional theory for molecules and molecular solids, *J. Mol. Struct.*, 2009, **914**, 3.
- 43 C. A. Ullrich, *Time-Dependent Density-Functional Theory: Concepts and Applications*, Oxford University Press, UK, 2012, pp. 145–151.
- 44 C. Wang, J. Shao, F. Chen and X. Sheng, Excited-state absorption for zinc phthalocyanine from linear-response time-dependent density functional theory, *RSC Adv.*, 2020, **10**, 28066.
- 45 H. Zhu, J. Wang, F. Wang, E. Feng and X. Sheng, Linear and quadratic response TDDFT methods for the excited-state absorption in oligofluorenes, *Chem. Phys. Lett.*, 2021, **785**, 139150.
- 46 Z. Liu, B. Zhang, N. Dong, J. Wang and Y. Chen, Perfluorinated gallium phthalocyanine axially grafted black phosphorus nanosheets for optical limiting, *J. Mater. Chem. C*, 2020, **8**, 10197.
- 47 T. Wang, W. Huang, T. Sun, W. Zhang, W. Tang, L. Yan, J. Si and H. Ma, Two-dimensional metal-polyphthalocyanine conjugated porous frameworks as promising optical limiting materials, *ACS Appl. Mater. Interfaces*, 2020, **12**, 46565.
- 48 K. Ishii and N. Sakai, Wavelength-tunable excited-state absorption and optical limiting effects in the Q band region based on silicon phthalocyanine oligomers, *Phys. Chem. Chem. Phys.*, 2010, **12**, 15354.
- 49 M. J. Frisch, G. W. Trucks, H. B. Schlegel, G. E. Scuseria, M. A. Robb, J. R. Cheeseman, G. Scalmani, V. Barone, B. Mennucci and G. A. Petersson, *et al.*, *Gaussian 09, Revision D.01*, Gaussian, Inc., Wallingford, CT, 2009.
- 50 T. Lu, *Molclus program, Version 1.9.9.4*, <https://www.keinsci.com/research/molclus.html>, (accessed on Jun 28, 2021).
- 51 J. J. P. Stewart, *MOPAC2016, Version 21.238L*, *Stewart Computational Chemistry*, Colorado Springs, CO, USA, <https://OpenMOPAC.net/>.
- 52 M. W. Schmidt, K. K. Baldridge, J. A. Boatz, S. T. Elbert, M. S. Gordon, J. H. Jensen, S. Koseki, N. Matsunaga, K. A. Nguyen and S. Su, *et al.*, General atomic and molecular electronic structure system, *J. Comput. Chem.*, 1993, **14**, 1347.
- 53 K. Aidas, C. Angeli, K. L. Bak, V. Bakken, R. Bast, L. Boman, O. Christiansen, R. Cimiraglia, S. Coriani and P. Dahle, *et al.*, The Dalton quantum chemistry program system, *Wiley Interdiscip. Rev.: Comput. Mol. Sci.*, 2014, **4**, 269.
- 54 K. Aidas, C. Angeli, K. L. Bak, V. Bakken, R. Bast, L. Boman, O. Christiansen, R. Cimiraglia, S. Coriani and P. Dahle, *et al.* Dalton, a Molecular Electronic Structure Program, Release Dalton 2018.alpha (2018), see <https://daltonprogram.org>.
- 55 T. Lu and F. Chen, Multiwfn: A Multifunctional Wavefunction Analyzer, *J. Comput. Chem.*, 2012, **33**, 580.
- 56 T. Lu, Multiwfn - A Multifunctional Wavefunction Analyzer - Software Manual (section 3.21.8).
- 57 J. Zhang and T. Lu, Efficient evaluation of electrostatic potential with computerized optimized code, *Phys. Chem. Chem. Phys.*, 2021, **23**, 20323.
- 58 W. Humphrey, A. Dalke and K. Schulten, VMD: Visual molecular dynamics, *J. Mol. Graphics*, 1996, **14**, 33.
- 59 J. Gierschner, H. G. Mack, L. Luer and D. Oelkrug, Fluorescence and absorption spectra of oligophenylenevinyls: Vibronic coupling, band shapes, and solvatochromism, *J. Chem. Phys.*, 2002, **116**, 8596.
- 60 M. Rumi, J. E. Ehrlich, A. A. Heikal, J. W. Perry, S. Barlow, Z. Hu, D. McCord-Maughon, T. C. Parker, H. Röckel and S. Thayumanavan, *et al.*, Structure-property relationships for two-photon absorbing chromophores: Bis-donor diphenylpolyene and bis(styryl)benzene derivatives, *J. Am. Chem. Soc.*, 2000, **122**, 9500.
- 61 S. J. K. Pond, O. Tsutsumi, M. Rumi, O. Kwon, E. Zojer, J.-L. Brédas, S. R. Marder and J. W. Perry, Metal-ion sensing fluorophores with large two-photon absorption cross sections: Aza-crown ether substituted donor-acceptor-donor distyrylbenzenes, *J. Am. Chem. Soc.*, 2004, **126**, 9291.
- 62 K. Zhao, L. Ferrighi, L. Frediani, C.-K. Wang and Y. Luo, Solvent effects on two-photon absorption of dialkylamino substituted distyrylbenzene chromophore, *J. Chem. Phys.*, 2007, **126**, 204509.
- 63 N. M. B. Neto, L. De Boni, C. R. Mendonca, L. Misoguti, S. L. Queiroz, L. R. Dinelli, A. A. Batista and S. C. Zilio, Nonlinear absorption dynamics in tetrapyrrolyl metalloporphyrins, *J. Phys. Chem. B*, 2005, **109**, 17340.
- 64 H. Xu, S. Q. Zhao, Y. Ren, W. Xu, D. B. Zhu, J. Z. Jiang and J. F. Cai, Primary investigation of the optical limiting performance of cyclo[8]pyrrole with a wide optical limiting window, *RSC Adv.*, 2016, **6**, 21067.
- 65 J. Xu, J. Chen, L. Chen, R. Hu, S. Wang, S. Li, J. S. Ma and G. Yang, Enhanced optical limiting performance of substituted metallo-naphthalocyanines with wide optical limiting window, *Dyes Pigm.*, 2014, **109**, 144.
- 66 F. C. Spano, Absorption and emission in pinwheel aggregates of oligo-phenylene vinylene molecules, *J. Chem. Phys.*, 2001, **114**, 5376.
- 67 N. Kobayashi, Dimers, trimers and oligomers of phthalocyanines and related compounds, *Coord. Chem. Rev.*, 2002, **227**, 129.